Markov Chain Modeling of Chaotic Wandering in Simple Coupled Chaotic Circuits

Yoshifumi NISHIO*†, Martin HASLER* and Akio USHIDA†

Abstract — **In this study, chaotic wandering phenomenon observed in simple coupled chaotic circuits is modeled by Markov chains. As coupling parameter increases, the solution of the coupled chaotic circuits starts to wander chaotically over 6 different phase states which are stable for smaller value of the parameter. The wandering is modeled by first-order and second-order Markov chains with the 6 states plus 3 intermediate states. Stationary probability distribution, expected sojourn time and probability density function of sojourn time are calculated from transition probabilities. These statistical quantities are compared with those obtained from computer simulations.**

1 Introduction

Spatio-temporal phenomena observed from coupled chaotic systems attract many researchers' attentions. For discrete-time mathematical models, there have been numerous excellent results. Kaneko's coupled map lattice is the most interesting and well-studied system [1]. He discovered various nonlinear spatio-temporal chaotic phenomena such as clustering, Brownian motion of defect and so on. Also Aihara's chaos neural network is the most important chaotic network from an engineering point of view [2]. His study indicated new possibility of engineering applications of chaotic networks, namely dynamical search of patterns embedded in neural networks utilizing chaotic wandering. Further, application of chaos neural network to optimization problems is widely studied. However, chaotic wanderings in continuous-time circuits have not been studied well. Therefore, in order to fill the gap between studies of discrete-time mathematical abstract and studies of continuous-time real physical systems, it is important to investigate simple continuous-time coupled chaotic circuits generating chaotic wandering, clustering, pattern switching, and so on.

We have proposed continuous-time coupled chaotic circuits systems and have investigated generating spatial patterns and chaotic wandering of spatial patterns [3]. In our latest studies, we have reported similar coupled circuits could generate chaotic wandering over several phase states characterized by four-phase synchronization and have shown that dependent variables corresponding to the angles of the solutions in subcircuit were useful to grasp the complicated phenomena [4][5]. The important feature of our coupled circuits is their coupling structure. Namely, adjacent four chaotic circuits are coupled by one resistor. Because such a coupling exhibited quasi-synchronization with phase difference [6], various spatial patterns could be generated. It would be followed by generation of several complicated spatio-temporal chaotic phenomena observed in discrete-time mathematical models. Therefore, the network based on the coupled circuits would be a good model to make clear physical mechanism of spatio-temporal chaotic phenomena in continuous-time systems. However, because it is extremely difficult to treat higher-dimensional nonlinear phenomena in continuous-time systems theoretically, we have to develop several tools to reveal the essence of the complicated phenomena.

In this study, chaotic wandering phenomenon observed in four simple chaotic circuits coupled by one resistor is modeled by Markov chains. The circuits exhibit four-phase synchronization of chaos for relatively small coupling parameter values. Because of the symmetry of the coupling, there coexist 6 different phase states. As the coupling parameter increases, the solution starts to wander chaotically over the 6 different phase states which are stable for smaller value of the parameter. The wandering is modeled by first-order and second-order Markov chains with the 6 states plus 3 intermediate states. Transition probabilities between the states can be obtained by counting all of the transitions in plenty of computer simulation. Stationary probability distribution, expected sojourn time and probability density function of sojourn time are calculated from the transition probabilities. These statistical quantities are compared with those obtained from computer simulations.

2 Circuit Model

Figure 1 shows four coupled chaotic circuits. The $i-v$ characteristics of the diodes are approximated by a two-segment piecewise-linear function as

$$v_d(i_k) = 0.5\,(r_d\,i_k + E - |\,r_d\,i_k - E\,|\,). \qquad (1)$$

By changing the variables and parameters,

$$I_k = \sqrt{C/L_1}E\,x_k, \quad i_k = \sqrt{C/L_1}E\,y_k, \quad v_k = E\,z_k,$$
$$t = \sqrt{L_1C}\,\tau, \quad \alpha = L_1/L_2, \quad \beta = r\sqrt{C/L_1},$$
$$\gamma = R\sqrt{C/L_1}, \quad \delta = r_d\sqrt{C/L_1}, \qquad (2)$$

*Laboratory of Nonlinear Systems, Department of Communication Systems, Swiss Federal Institute of Technology Lausanne, EL-Ecublens, CH-1015 Lausanne, Switzerland. E-mail: nishio@circpc.epfl.ch, martin.hasler@epfl.ch.

†Department of Electrical and Electronic Engineering, Tokushima University, 2-1 Minami-Josanjima, Tokushima 770-8506, Japan. E-mail: nishio@ee.tokushima-u.ac.jp, ushida@ee.tokushima-u.ac.jp, Tel: +81-88-656-7470, Fax: +81-88-656-7471.

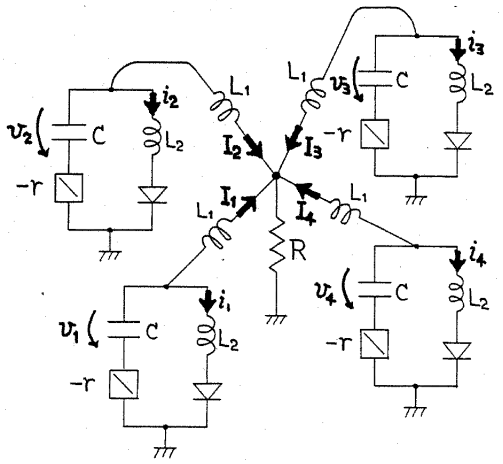

Figure 1: Circuit model.

the normalized circuit equations are given as

$$\begin{cases} \dfrac{dx_k}{d\tau} &= \beta(x_k + y_k) - z_k - \gamma \displaystyle\sum_{j=1}^{4} x_j \\ \dfrac{dy_k}{d\tau} &= \alpha\{\beta(x_k + y_k) - z_k - f(y_k)\} \\ \dfrac{dz_k}{d\tau} &= x_k + y_k \qquad (\ \mathrm{k}= 1, 2, 3, 4\ ) \end{cases} \tag{3}$$

where

$$f(y_k) = 0.5\ (\delta\ y_k + 1 - |\ \delta\ y_k - 1\ |\ ). \tag{4}$$

3 Four-Phase Synchronization and Chaotic Wandering

Figure 2 shows an example of the observed four-phase synchronizations. Though only circuits experimental results are shown, similar results can be obtained by computer calculations. In the figures the phase differences of I_2, I_3 and I_4 with respect to I_1 are almost 90°, 180° and 270°, respectively. However, because of the symmetry of the coupling structure, six different combinations of phase states coexist.

Further, we can observe chaotic wandering of the 6 phase states of the four-phase synchronization by tuning coupling parameter value. In order to investigate the chaotic wandering, we define the Poincaré section as $z_1 = 0$ and $x_1 < 0$. Further we define the following independent variables from the discrete data of $x_k(n)$ and $z_k(n)$ on the Poincaré map.

$$\varphi_k(n) = \begin{cases} \pi - \tan^{-1} \dfrac{z_{k+1}(n)}{x_{k+1}(n)} & (x_{k+1}(n) > 0) \\ \pi + \tan^{-1} \dfrac{z_{k+1}(n)}{x_{k+1}(n)} & (x_{k+1}(n) < 0) \end{cases} \tag{5}$$

$$(\ \ k{=}1,\ 2,\ 3.\ \ )$$

Because the attractor observed from each subcircuit is strongly constrained onto the plane $y_k = 0$ when the diode is off, these variables can correspond to the phase differences between the subcircuit 1 and the others. (Note that the argument of the point $(x_1(n), z_1(n))$ is always π.) Figure 3 shows time evolution of $\varphi_k(n)$ when chaotic wandering occurs. We can see that several switchings of the phase difference appear in an irregular manner.

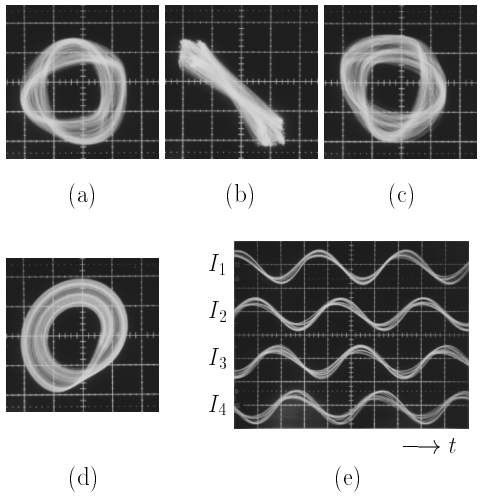

Figure 2: Four-phase synchronization of chaos. L_1=100.7mH, L_2=10.31mH, C=34.9nF, r=334Ω and R=198Ω. (a) $I_1 - I_2$. (b) $I_1 - I_3$. (c) $I_1 - I_4$. (d) $I_1 - v_1$.

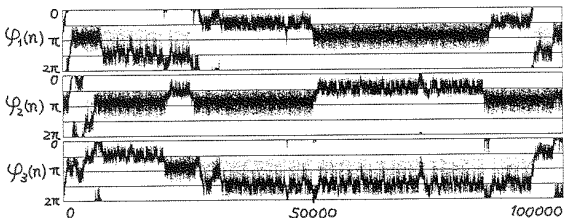

Figure 3: Chaotic wandering of phase states ($\alpha = 7.0$, $\beta = 0.13$, $\gamma = 0.46$ and $\delta = 100.0$).

4 Markov Chain Modeling of Chaotic Wandering

In this study the chaotic wandering observed in our circuit is modeled by Markov chains. It gives various statistical characteristics of the higher-dimensional nonlinear phenomenon and would help to carry out further detailed analysis.

At first, let us define the 6 phase states of the four-phase synchronization concretely using the variables in (5) as

$$\begin{array}{lcl} S_1 & : & \varphi_1 > \varphi_2 > \varphi_3 \\ S_2 & : & \varphi_1 > \varphi_3 > \varphi_2 \\ S_3 & : & \varphi_2 > \varphi_1 > \varphi_3 \\ S_4 & : & \varphi_2 > \varphi_3 > \varphi_1 \\ S_5 & : & \varphi_3 > \varphi_1 > \varphi_2 \\ S_6 & : & \varphi_3 > \varphi_2 > \varphi_1. \end{array} \tag{6}$$

By careful investigation of the behavior of the solutions around switchings between two of the above 6 phase states, we found that the solution often stays in intermediate phase states during a certain

period. In the intermediate phase states, 2 of the four circuits are almost synchronized at in-phase and the rest are also synchronized at in-phase with π-phase difference against the former pair (like in- and opposite-phases quasi-synchronization in [3]). These phase states can be characterized by

$$\begin{array}{lcl} S_{I1} & : & |\varphi_1 - \pi| < \theta_I \quad \cap \quad |\varphi_2 - \varphi_3| < \theta_I \\ S_{I2} & : & |\varphi_2 - \pi| < \theta_I \quad \cap \quad |\varphi_1 - \varphi_3| < \theta_I \\ S_{I3} & : & |\varphi_3 - \pi| < \theta_I \quad \cap \quad |\varphi_1 - \varphi_2| < \theta_I \end{array} \tag{7}$$

where θ_I is a parameter deciding largeness of the region of the intermediate phase states. Note that the condition of the decision of the phase states (6) should be modified because of introducing these intermediate phase states.

Next, let us consider a state-transition diagram representing the transitions between the above-mentioned phase states $S_1 - S_6$ and $S_{I1} - S_{I3}$. By virtue of the symmetry of the coupling of the original system, we have to consider only S_1 and S_{I1}. Figure 4 shows a part of the state-transition diagram focusing on the phase state S_1 where

$$P_1 = 1 - \sum_{i=2}^{7} P_i. \tag{8}$$

Note that the paths from S_1 to S_6 and to S_I2 do not exist, because these transitions need double switching beyond one of the other phase states which was very rare in our computer simulations. Figure 5 shows a part of the state-transition diagram focusing on the intermediate phase state S_{I1} where

$$P_8 = 1 - 2(P_9 + P_{10}). \tag{9}$$

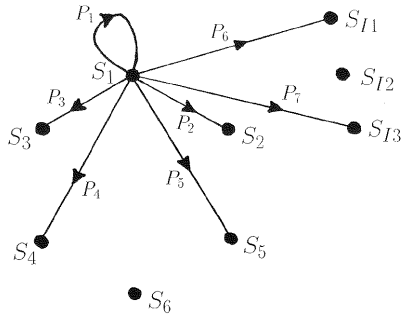

Figure 4: State-transition diagram I (only transitions from S_1).

From the whole state-transition diagram, we can get the transition probability matrix $\hat{\mathbf{P}}$ as

$$\begin{bmatrix} P_1 & P_2 & P_3 & P_5 & P_4 & 0 & P_9 & 0 & P_{10} \\ P_2 & P_1 & P_4 & 0 & P_3 & P_5 & P_9 & P_{10} & 0 \\ P_3 & P_5 & P_1 & P_2 & 0 & P_4 & 0 & P_9 & P_{10} \\ P_4 & 0 & P_2 & P_1 & P_5 & P_3 & P_{10} & P_9 & 0 \\ P_5 & P_3 & 0 & P_4 & P_1 & P_2 & 0 & P_{10} & P_9 \\ 0 & P_4 & P_5 & P_3 & P_2 & P_1 & P_{10} & 0 & P_9 \\ P_6 & P_6 & 0 & P_7 & 0 & P_7 & P_8 & 0 & 0 \\ 0 & P_7 & P_6 & P_6 & P_7 & 0 & 0 & P_8 & 0 \\ P_7 & 0 & P_7 & 0 & P_6 & P_6 & 0 & 0 & P_8 \end{bmatrix}. \tag{10}$$

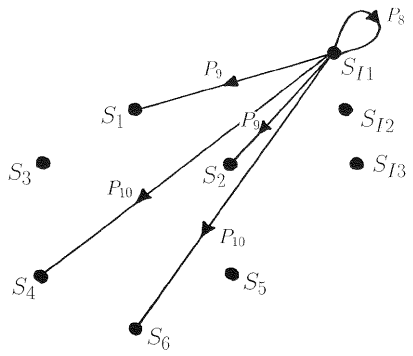

Figure 5: State-transition diagram II (only transitions from S_{I1}).

The stationary probability distribution describing probability of the solution being in each phase state;

$$\mathbf{Q} = [Q_{S_1}, Q_{S_2}, \cdots, Q_{S_{I3}}]^T \tag{11}$$

can be calculated from the following equations

$$\mathbf{Q} = \mathbf{PQ} \quad \text{and} \quad \sum_{i=1}^{6} Q_{S_i} + \sum_{j=1}^{3} Q_{S_{Ij}} = 1. \tag{12}$$

It is also possible to estimate expected sojourn time in each phase state by using the transition probabilities. For example, probability density function of the sojourn time in S_1 is given by

$$P_{ST}(S_1, n) = P_1^{n-1}(1 - P_1). \tag{13}$$

From (13) the expected sojourn time in S_1 is calculated as

$$\begin{aligned} E_{ST}(S_1) &= \sum_{n=1}^{\infty} \{n \times P_{ST}(S_1, n)\} \\ &= (1 - P_1) \sum_{n=1}^{\infty} n P_1^{n-1} \\ &= \frac{1}{1 - P_1}. \end{aligned} \tag{14}$$

In order to get more accurate statistical information of the phenomena, we also model the phenomenon by second-order Markov chain. In this case, the transition probability matrix becomes 57×57 and the probability density function of the sojourn time becomes a little bit complicated.

5 Results and Discussions

Table 1 shows the stationary probabilities and the expected sojourn times obtained from computer simulation, first-order Markov chain and second-order Markov chain. Computer simulations were carried out over 10,000,000 iterations of the Poincaré map. Transition probabilities of the Markov chains are obtained by counting all of transitions during the computer simulations. We can see the results obtained from both of the first-order Markov chain and the second-order one agree very well with computer simulated results.

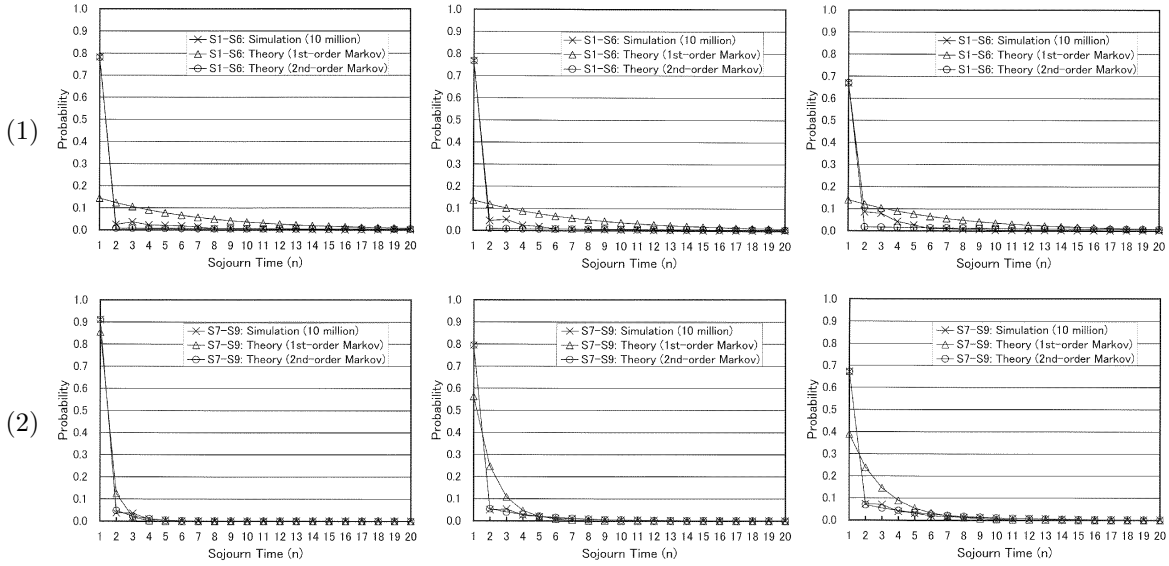

Figure 6: Probability density functions of sojourn time ($\alpha = 7.0$, $\beta = 0.13$, $\gamma = 0.50$ and $\delta = 100.0$). (a) $\theta_I = \pi/12$. (b) $\theta_I = \pi/6$. (c) $\theta_I = \pi/4$. (1) $S_1 - S_6$. (2) $S_{I1} - S_{I3}$.

Table 1: Stationary probabilities Q and expected sojourn times E_{ST} ($\alpha = 7.0$, $\beta = 0.13$, $\gamma = 0.50$ and $\delta = 100.0$).

θ_I		Sim.	Markov (1st)	Markov (2nd)
$\frac{\pi}{12}$	$Q_{S_1-S_6}$	0.1633	0.1633	0.1631
	$Q_{S_{I1}-S_{I3}}$	0.0068	0.0068	0.0071
	$E_{ST}(S_{1-6})$	7.009	7.002	7.050
	$E_{ST}(S_{I1-I3})$	1.170	1.170	1.170
$\frac{\pi}{6}$	$Q_{S_1-S_6}$	0.1536	0.1536	0.1536
	$Q_{S_{I1}-S_{I3}}$	0.0261	0.0261	0.0262
	$E_{ST}(S_{1-6})$	7.326	7.319	7.324
	$E_{ST}(S_{I1-I3})$	1.778	1.778	1.779
$\frac{\pi}{4}$	$Q_{S_1-S_6}$	0.1357	0.1357	0.1357
	$Q_{S_{I1}-S_{I3}}$	0.0619	0.0619	0.0619
	$E_{ST}(S_{1-6})$	7.139	7.135	7.137
	$E_{ST}(S_{I1-I3})$	2.566	2.566	2.566

Figure 6 shows the probability density functions of the sojourn time. From the figures, we can say that the first-order Markov chain could not explain the chaotic wandering phenomenon in our system correctly. On the other hand, the second-order Markov chain displays better agreement especially for the intermediate states $S_{I1} - S_{I3}$ (Fig. 6(2)). We have to mention that error for $S_1 - S_6$ around $n = 2, 3$ increases as θ_I increases (Fig. 6(1c)). This error is considered to be caused by unneglectable higher-order Markov property. Investigating the relationship between the error and the order of the Markov chains is our important future problem.

6 Conclusions

In this study, chaotic wandering phenomenon observed in four simple chaotic circuits coupled by one resistor has been modeled by first-order and second-order Markov chains with 6 original states plus 3 intermediate states. Stationary probability distribution, expected sojourn time and probability density function of sojourn time have been calculated from the transition probabilities. By comparing these statistical quantities with those obtained from computer simulations, We have the results that the first-order Markov chain can not explain the phenomenon correctly and that the second-order Markov chain could explain the phenomenon efficiently. We consider that the result of this study would help to analysis chaotic wandering in continuous-time circuits in detail.

References

[1] K. Kaneko (ed.), *Theory and Applications of Coupled Map Lattices*, John Wiley & Sons, Chichester, 1993.

[2] K. Aihara, T. Takabe and M. Toyoda, "Chaotic Neural Networks," *Phys. Lett. A*, vol. 144, no. 6&7, pp. 333–340, 1990.

[3] Y. Nishio and A. Ushida, "Spatio-Temporal Chaos in Simple Coupled Chaotic Circuits," *IEEE Trans. Circuits Syst. I*, vol. 42, no. 10, pp. 678–686, Oct. 1995.

[4] Y. Nishio and A. Ushida, "On Phase Pattern in a Two-Dimensional Coupled Chaotic Circuits Network," *Proc. NOLTA'98*, vol. 1, pp. 31-34, Sep. 1998.

[5] Y. Nishio and A. Ushida, "Analysis of Chaotic Wandering of Phase Patterns in a Two-Dimensional Coupled Chaotic Circuits Network," *Proc. ISCAS'99*, vol. 5, pp. 422-425, May 1999.

[6] Y. Nishio and A. Ushida, "Quasi-Synchronization Phenomena in Chaotic Circuits Coupled by One Resistor," *IEEE Trans. Circuits Syst. I*, vol. 43, no. 6, pp. 491–496, Jun. 1996.